Vol. 530: 77–92, 2015
doi: 10.3354/meps11289

MARINE ECOLOGY PROGRESS SERIES
Mar Ecol Prog Ser

Published June 18

Effect of monsoonal perturbations on the occurrence of phytoplankton blooms in a tropical bay

Jagadish S. Patil, Arga Chandrashekar Anil*

CSIR — National Institute of Oceanography, Dona Paula, 403 004 Goa, India

ABSTRACT: In this study, the influence of intraseasonal variations in rainfall and the resultant freshwater flux (monsoon perturbations) on phytoplankton bloom dynamics were evaluated by quantifying live phytoplankton at a fixed station (Dona Paula Bay, west coast of India) every day during the 2008 southwest monsoon season (June–September). Pre-processing of the sample for live phytoplankton analysis using FlowCAM through fluorescence-based quantification of phytoplankton size fractions is described for the first time. Six diatom blooms of autochthonous origin were encountered during the observations, coinciding with nutrient enrichment and a lull in river runoff. The blooms observed at the beginning (1st bloom) and the end of the season (6th bloom) were dominated by nano- and picophytoplankton, and the intervening blooms by microphytoplankton. All blooms coincided with flood tide or high tide under optimal salinity (>15) and light (depth of light penetration: >50 cm; solar radiation: 30–70 mW cm^{-2}) conditions following heavy rainfall and nutrient flux. Termination of blooms coincided with nitrate exhaustion. Dinoflagellate (2nd dominant group) abundance was positively associated with depth of light penetration >100 cm and low nutrient concentrations. Bloom duration of 1–6 d was recorded, indicating that such events are widespread and can significantly influence the system's metabolic balance. The average net photic zone production of the season was positive (0.11 ± 0.67 g O_2 m^{-2} d^{-1}), and a quarter of the monsoon season was net autotrophic. Although bloom production was underutilized (up to 63%), much of the system's carbon requirement (up to 70%) was met by allochthonous supply.

KEY WORDS: Tropical bay · FlowCAM · Phytoplankton · Diatoms · Dinoflagellates · Blooms · Monsoon

INTRODUCTION

Phytoplankton abundance and species composition in estuarine ecosystems are closely linked to various physical (advection, light, temperature, salinity, etc.), chemical (pH, nutrients) and biological (grazing) factors as well as interactions among them (Pennock 1985, Cole et al. 1992, Lehman 1992, Cloern 1996, Irigoien & Castel 1997, Sin et al. 1999, Underwood & Kromkamp 1999, Cloern & Jassby 2010, Zingone et al. 2010, Lawrenz et al. 2013). The continual documentation of phytoplankton population dynamics with relevant environmental variables can provide information on the functioning of an ecosystem. The phytoplankton community, a source of organic carbon and energy for higher trophic levels, ultimately determines the nature of fishery production. Understanding phytoplankton dynamics is therefore central to understanding how estuarine ecosystems work and how they respond to environmental stresses imposed by natural and anthropogenic activities (Cloern 1979). A 4-decade long study in San Francisco Bay has shown the importance of environmental monitoring in identifying the causes of changes in ecosystem functioning as well as for establishing and measuring outcomes of environmental policies that aim to maintain high water quality and sustain services provided by estuarine-coastal ecosystems (Cloern & Jassby 2012).

The estuaries in the Indian subcontinent are influenced by the southwest monsoon (SWM) rainfall dur-

*Corresponding author: acanil@nio.org

ing June to September and are therefore categorized among the most remarkable estuaries when compared with better-studied estuaries (e.g. San Francisco Bay, Chesapeake Bay, Delaware Bay, Columbia River estuary, European estuaries) in extra-tropical regions (Vijith et al. 2009). The distinguishing feature of the monsoonal estuaries compared to better-studied estuaries is the high annual runoff and a distinctly higher runoff during monsoon season (wet season) compared to the non-monsoon season, i.e. dry season (Vijith et al. 2009). Such typical alternating wet and dry seasons are also observed in other parts of Asia that experience a monsoon climate, as well as subtropical South America and parts of Australia and South Africa (e.g. Eyre 2000, Murrell et al. 2007, Vijith et al. 2009, Sin et al. 2012).

The SWM brings in heavy precipitation (250 to 300 cm yr^{-1}) in this part of the world and is known to influence the functioning of tropical estuarine systems and the adjoining regions by enforcing environmental perturbations. Increased flux of nutrients and suspended solids from land, as well as the intensifying anoxia on the western Indian continental shelf (Naqvi et al. 2000), are some of the instances of perturbations. Besides river water as a source, ground water, atmospheric transport and benthic flux are known to affect patterns of nutrient inputs into estuaries (Nowicki & Nixon 1985, Malone et al. 1988, Paerl 1997, Conley 2000, Sarma et al. 2010). All these environmental perturbations are known to affect patterns of organic production, distribution of organisms, food webs, chemical fluxes, benthic-pelagic coupling, etc. (e.g. Eyre & Ferguson 2006, Sarma et al. 2009, 2010, Patil & Anil 2011, Vinagre et al. 2011, Acharyya et al. 2012). Phytoplankton, which are important for the functioning of estuarine ecosystems and the adjoining seas, respond quickly to such environmental perturbations. In recent years, with concern over the global increase in harmful algal blooms (HABs), studies related to the dynamics of phytoplankton populations have gained further importance. Until recently, in algal bloom monitoring programs, phytoplankton analysis was based upon cell counts using microscopy. However, microscope cell-counting requires fixation, and available techniques for optimal preservation and enumeration of phytoplankton are taxon-specific (Zarauz & Irigoien 2008 and references therein). Enumeration of live phytoplankton will thus be useful in overcoming this limitation. Taking this into consideration, we observed phytoplankton bloom dynamics based on live cell monitoring (using FlowCAM) and the environmental settings influencing them by carrying out observations in Dona Paula Bay (see Fig. 1) during the SWM season of 2008. Personal observations indicated that naked dinoflagellates (including HAB species) are known to occur in high numbers during or immediately after the monsoon in the study region, and it is important to document the same.

Dona Paula Bay, located on the west coast of India, in Goa, is a semi-enclosed bay located at the mouth of the Zuari estuary. The river Zuari has its origin in the Western Ghats, and it extends up to 70 km before meeting the Arabian Sea. The Zuari estuary is referred to as a 'monsoonal estuary' as it is influenced by the summer monsoon (i.e. the SWM) during June to September (Vijith et al. 2009). During this period, the hydrodynamics of the estuary are controlled by physics (natural patterns of river runoff and tides), and the changes associated with the onset of the monsoon have marked effects on the physico-chemical nature of the water, phytoplankton community, food web and production (Bhattathiri et al. 1976, Qasim & Sen Gupta 1981, Devassy & Goes 1988, Patil & Anil 2011, Rao et al. 2011). Earlier studies (Devassy & Goes 1988, Krishnakumari et al. 2002) using low-resolution sampling in this estuary, but slightly upstream from the station used in the present study, revealed a minimum in cell abundance during the SWM seasons in 1980 and 1998, and attributed this to poor growth conditions (such as lowered light and salinity regimes caused by monsoon events) and the absence of species that can bloom under such conditions. However, some later studies (Mitbavkar & Anil 2002, Patil & Anil 2008) in the study area have reported *Skeletonema* blooms during the SWM season under low saline conditions in the same system, as well as elsewhere along the west coast of India. Patil & Anil (2011) also reported mixed-species blooms of diatoms and dinoflagellates under high saline conditions during a break period in the monsoon. Such contrasting results indicate intraseasonal variations (e.g. number of bloom events, duration of the bloom, bloom-causing species and the environmental factors causing blooms). Such variations can be captured only through high-resolution sampling, and this is addressed in the present study. Phytoplankton samples, along with related environmental parameters, were collected every 24 h from a fixed station in Dona Paula Bay. In addition, production and respiration measurements were also made at regular intervals in order to understand the metabolic status of the plankton. Currently, the seasonal metabolic status of the water column from the Mandovi–Zuari estuarine system is available (Ram et al. 2003). However, describing the patterns in the occurrence of blooms

during different periods of the SWM would improve our understanding of the interactions between the monsoon and phytoplankton activity.

MATERIALS AND METHODS

Study site

Surface water samples were collected using a bucket from 28 May to 30 September 2008 in Dona Paula Bay (average depth: 3 m at the station) at a fixed location (15° 25′ N, 73° 59′ E; Fig. 1a) between 11:00 and 12:00 h. Thus, the sampling occurred at different phases of the tide and river discharge (Fig. 1b,c). During the study period, tidal amplitude ranged from a low of −0.24 m to a high of 2.22 m, and the calculated tidal amplitude at the time of sampling ranged from 1.05 to 2.22 m (Fig. 1b). The sampling time was fixed to avoid the complexity of diurnal changes in the biogeochemical properties while comparing the data.

Water sampling

The temperature of the collected water sample was measured *in situ* at the time of sampling. The depth of light penetration was measured using a Secchi disc. Salinity samples were analyzed by using a salinometer (AUTOSAL 8400A). Dissolved oxygen (DO) was measured following standard procedures (Parsons et al. 1984). Oxygen saturation was calculated using temperature, salinity and DO values (Benson & Krause 1984). Nutrients (NH_4, NO_3-N, NO_2-N, PO_4-P and SiO_3) were analyzed once every 3 d following standard procedures (Parsons et al. 1984). Turbidity of the samples was measured in the laboratory using a Trilogy fluorometer (Turner Designs) equipped with a turbidity module. Primary productivity (PP) was also measured by the DO method at regular intervals (approximately once every 3 d) during the investigation period. For PP measurements, 2 sets of biological oxygen demand (BOD) glass bottles, 1 each for light and dark conditions, were incubated by suspension for 24 h in a pond located on the premises. Due to very rough conditions, it was not possible for us to incubate the bottles at the study site; hence we selected an aquaculture pond in the premises of CSIR — National Institute of Oceanography (CSIR-NIO), which is close to the bay. The water transparency level (Secchi disc depth of 1–1.5 m) and water temperature (±1–2°C) of the pond were almost of the same magnitude as that of the study location. The dark bottles were wrapped with black tape and aluminum foil. The DO in both light- and dark-incubated samples were fixed immediately upon retrieval after 24 h and analyzed in the laboratory. The changes in DO concentrations in light and dark bottles between the initial measurement and after incubation were used to quantify net community production (NCP) and community respiration (CR). Gross primary production (GPP) was estimated as the sum of NCP and CR. Photic zone production and water column respiration were calculated by integrating the surface measurements over the photic depth (using Secchi disc measurements) and total water column, respectively. Surface GPP and NCP were integrated over the photic zone using the Secchi disc depth measurements (as, on most occasions, depth of light penetration was <2 m), whereas the column CR (CCR) was calculated by integrating CR to the total water column.

Chl *a* and size fractionation of chlorophyll fluorescence

A known volume (250 ml) of seawater was filtered through GF/F Whatman filter paper and the filter papers were immediately used for chl *a* analysis using the 90% acetone extraction method as described in Parsons et al. (1984). The fluorescence readings of the extracted chlorophyll were made on a Trilogy fluorometer (Turner Designs), equipped with a chlorophyll module. The same module was also used for the determination of size-fractioned chlorophyll fluorescence.

Phytoplankton size fractionation analysis was carried out with *in vivo* chlorophyll fluorescence measurements of the seawater samples (total fluorescence) and the samples filtered through a 20 µm mesh (nano- and picophytoplankton). The difference in the fluorescence reading gives the fluorescence of microphytoplankton. This method was used as there was a significant relationship between the *in vivo* fluorescence and the extracted chlorophyll measurements (total and size fractions; data not shown).

FlowCAM analysis

Identification of live phytoplankton was carried out using a factory-calibrated FlowCAM (Fluid Imaging Technologies) following a standard procedure in an auto-image mode using different magnifications (4× and 10×) and flow cells (300 and 100 µm) to capture

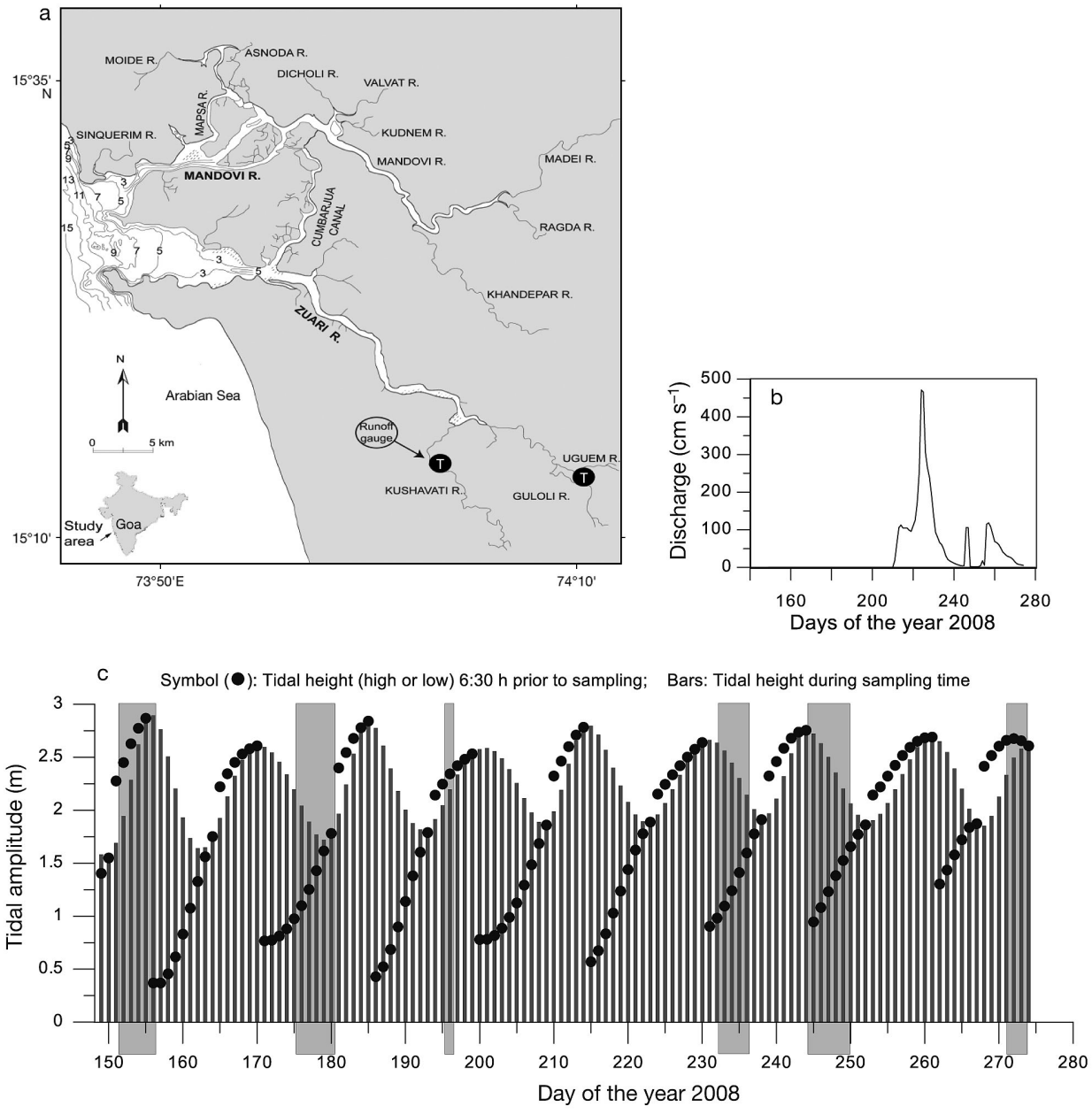

Fig. 1. (a) Location of the time series station in Dona Paula Bay, Goa, India. T in black dot indicates the location of a runoff gauge. Numbers in estuary mouth indicate depth (m). (b) Freshwater discharge from Guloli River. Generally, Zuari River receives fresh water from the 3 rivers (Kushavati, Uguem and Guloli) located upstream. The freshwater discharge data for only Guloli River is presented for the study period. (It is pertinent to note that Salauli Dam is built across the Guloli River and the discharge from this river occurs only when the water overflows. The discharge data for all 3 rivers for 2011 monsoon was available. Except at the beginning of the monsoon when the dam is yet to be filled up [for about a month], the pattern of discharge [highs and lows] from all the rivers is almost the same. For Guloli River, we account for nil discharge during early monsoon and up to 50–54 % during the rest of the season.) (c) Variations in tidal amplitude during sampling. The areas outlined in light gray represent periods of high chlorophyll

all phytoplankton size groups >5 µm. However, it should be noted that the analysis of natural samples with FlowCAM requires a planned preprocessing of the samples, not only to avoid cell clumping and obstruction to the flow chamber (Álvarez et al. 2011), but also to select the appropriate combination of flow cell and objective. Although FlowCAM is an advanced technology which has the ability to perform continuous recording of the images/data, one of the challenges with the system is optics, i.e. manual

selection of objectives and flow cells depending on the particle size present in a sample to be analyzed. Considering the heterogeneous size distribution of the microphytoplankton and the optical limitations of FlowCAM (appropriate selection of flow cells and objectives), the method used for the analysis of live microphytoplankton cells is described here. The method involves a systematic preprocessing of the samples to determine the dominance of microphytoplankton belonging to different size groups (<100 or >100 µm) in the natural sample to be analyzed. To the best of our knowledge, such an approach has not been described in earlier studies. The quantification of different size groups (<100 and >100 µm) from natural samples was performed by *in vivo* fluorescence measurements using Trilogy equipped with the chl *a* module. This method was adopted as it is non-destructive and easy and enables quick assessment. The quantification of different size fractions was achieved by the following procedure: (1) the fluorescence readings of the seawater sample were made, (2) an aliquot of the sample was passed through a 100 µm mesh, (3) the raw fluorescence values of the prefiltered sample were measured, and (4) if the fluorescence values of the seawater sample and the 100 µm prefiltered sample were the same, then the samples were analyzed using the 10× objective and 100 µm flow cell. In cases where the fluorescence values of the seawater sample were higher than those of the 100 µm prefiltered samples, then the samples were analyzed twice using 2 different combinations of objectives (10× and 4×) and flow cells (100 and 300 µm). The 10× objective and 100 µm flow cell combination was used to analyze the samples for the quantification of phytoplankton having <100 µm in size, whereas the 4× objective and the 300 µm flow cell were used for the quantification of phytoplankton >100 µm in size. Two to 5 ml of sample were analyzed. Invalid images, bubbles and repeated images were removed manually from the database. The identification of phytoplankton species was also carried out manually based on standard identification keys (Subrahmanyan 1959, Desikachary 1987, Round et al. 1990, Tomas 1997).

Meteorological parameters

Solar radiation and wind speed data were obtained from the Automatic Weather Station (AWS), CSIR-NIO, Goa, India. Data on rainfall and sunshine hours (the time of brightness [solar radiation > 1 mW cm^{-2}] available in day length) were obtained from the Indian Meteorological Department, Goa. For interpretation of these data, daily average values were used.

Statistical analyses

To evaluate the relationship between phytoplankton (both abundance and biomass) and environmental parameters, canonical correspondence analysis (CCA) and Spearman's rank correlation test were performed using the Multi-Variate Statistical Package (MVSP) version 3.1 and Statistica (release 5) programs, respectively. As the resolutions of nutrient data and other environmental data are not the same, 2 CCAs were performed. In CCA-1, the data on environmental parameters such as temperature, salinity, Secchi disc depth (depth of light penetration), turbidity, rainfall, solar radiation and DO collected daily were examined, whereas in CCA-2, nutrient data collected at 3 d intervals were used. Prior to statistical analysis, the heterogeneity in the biological data were removed by subjecting all data to $\log(x + 1)$ transformation. To further identify the optimal ranges of different environmental parameters for the occurrence of high chlorophyll and abundance (diatoms and dinoflagellates), a scatter diagram was plotted with different salinity ranges (on the *x*-axis) and corresponding values for each biological variables (on the *y*-axis), which were grouped into different levels based on the values of a given environmental parameter. For each biological variable, a total of 9 such diagrams were plotted by using tidal amplitude, temperature, Secchi disc depth, nitrate, phosphate, silicate, wind speed, rainfall and solar radiation as the grouping parameter.

RESULTS

Meteorological conditions

During the SWM period, the study region experiences high wind speed, low solar radiation and sunshine hours due to cloud cover, and maximum rainfall (Fig. 2a–c). During the study period, incidences of heavy rainfall were observed on 3 occasions, and the maximum rainfall received was 136 mm d^{-1} (Fig. 2a). Maximum wind speed (18 m s^{-1}) recorded was in the beginning of the SWM, with a subsequent decrease as the season progressed (Fig. 2c). Solar radiation (ranged between 49 to 67.3 mW cm^{-2}) and sunshine hours (variable with a maximum of 11 h) followed a similar trend (Fig. 2b,c).

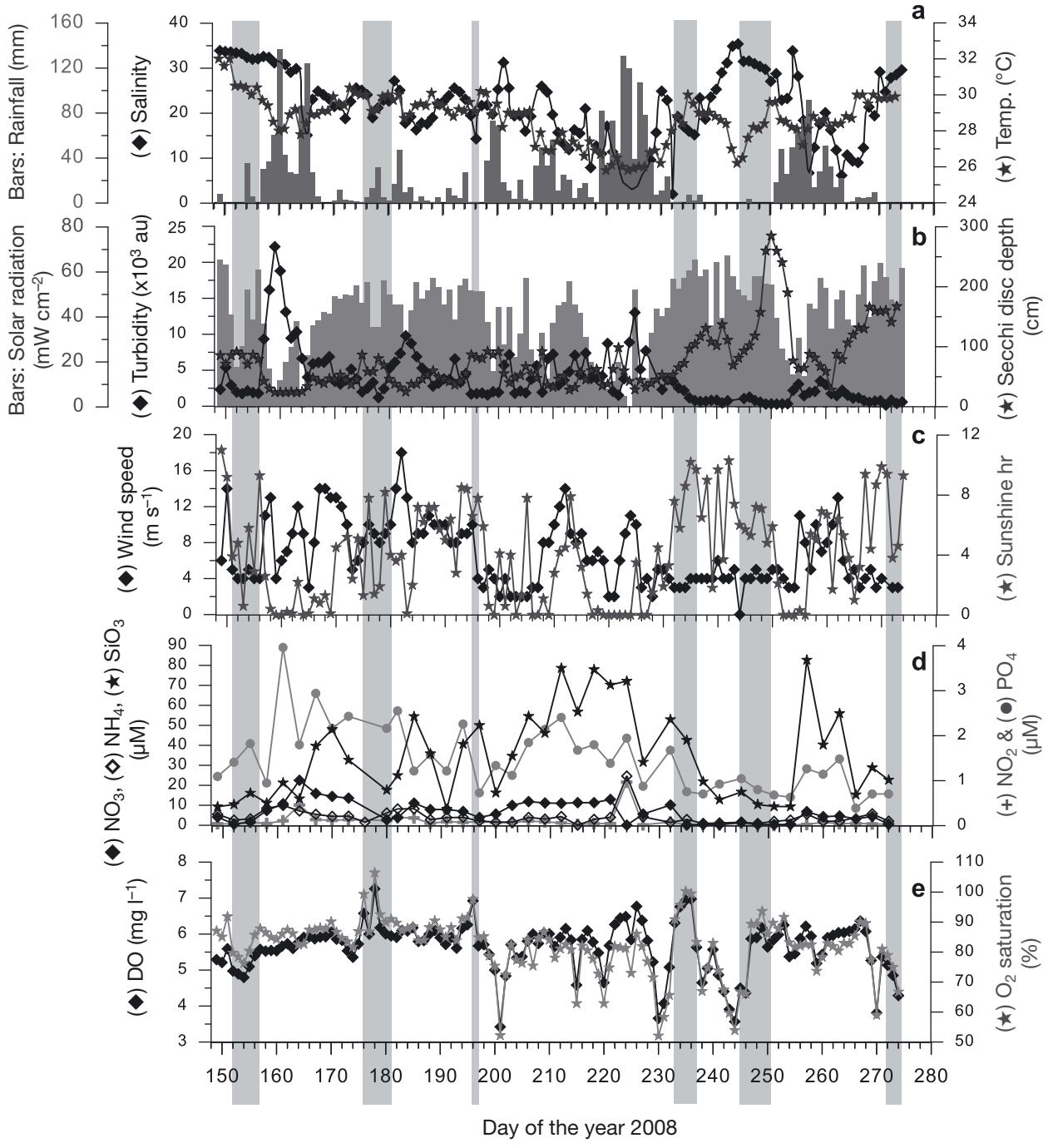

Fig. 2. Temporal variations in meteorological and environmental parameters during the 2008 southwest monsoon: (a) rainfall, temperature and salinity; (b) solar radiation, Secchi disc depth (depth of light penetration), and turbidity (au: arbitrary units); (c) wind speed and sunshine hours; (d) dissolved nutrients; and (e) dissolved oxygen (DO) and oxygen saturation. Shaded areas in light gray represent periods of chlorophyll peaks

Hydrographic conditions

Maximum surface seawater temperature (SST) was 32°C and the minimum was 25.8°C (Fig. 2a) during the study period. The data indicated that SST was >30°C before the onset of monsoon and <30°C during the rest of the season. Salinity dropped at the onset of monsoon, and intraseasonal variability influenced by the intensity of freshwater flux was evident (Fig. 2a).

Transparancy and turbidity (measured by Secchi disc and the turbidity module) varied significantly during the sampling period, with values ranging from 23.4 to 285 cm and 154 to 22 170 (arbitrary units, au), respectively (Fig. 2b). These 2 variables showed a significant inverse relationship (Fig. 2b). The depth of light penetration was low from the beginning to the middle of the season, but increased as the season progressed.

The variation in nutrient (NH_4, NO_3-N, NO_2-N, PO_4-P and SiO_3) concentrations showed that the nutrient inputs were introduced into the study region in pulses (Fig. 2d). Maximum concentrations of NO_3-N and PO_4-P were found during the early phase of the SWM. Variations in NO_2-N and NH_4 followed a similar trend. NH_4 ranged from 0.10 to 24.61 µM, NO_3-N ranged from 0.07 to 22.51 µM, NO_2-N ranged from 0.02 to 0.97 µM, PO_4-P ranged from 0.39 to 3.96 µM, and SiO_3 ranged from 8.06 to 82.67 µM (Fig. 2d). The DO concentrations and oxygen saturation ranged from 3.42 to 7.26 ml l^{-1} and 52.1 to 106.5%, respectively (Fig. 2e).

The metabolic rates, i.e. NCP, CR, and GPP, in the surface and photic zone exhibited large variations during the monsoon season (Fig. 3a–c). The ranges for NCP, GPP, and CR for surface waters were −1.66 to 1.88, 0.08 to 3.12, and 0.38 to 2.82 g O_2 m^{-3} d^{-1}, respectively, whereas in the photic zone, the ranges were −1.5 to 1.8, 0.02 to 4.3, and 0.15 to 4.5 g O_2 m^{-2} d^{-1} (data not shown), respectively. The total CCR in the study location ranged from 1.13 to 8.46 g O_2 m^{-2} d^{-1}, which is about 3.5 times (avg.) higher than the photic zone GPP. The NCP:GPP ratio, which is an indicator of exportable production, ranged from a low of −7.74 to a high of 0.63 (Fig. 3d), and high positive values were observed during bloom periods. In the photic zone, the GPP:CR ratio showed large variations, indicating a significant fluctuation in the trophic status (Fig. 3e), whereas the prevalence of a low GPP:CCR ratio (<1) indicated that net heterotrophic conditions prevailed in the water column throughout the study period.

Chl *a*, size-fractionated *in vivo* chlorophyll fluorescence and phytoplankton community

Chl *a* concentrations and *in vivo* chlorophyll fluorescence ranged from 0.27 to 8.97 µg l^{-1} and 322 to 5153 au, respectively, and showed a significant linear relationship ($n = 121$, $r = 0.896$, $p < 0.001$). Chlorophyll fluorescence revealed 6 peaks, indicating phytoplankton blooms (Fig. 4a). Fluorescence data indicated the maximum duration of a bloom to be 6 d. In addition to the high peaks, small peaks in chlorophyll concentrations were also observed. Size-fractionated chlorophyll fluorescence revealed that the contribution of <20 µm (nano- and picophytoplankton) and >100 µm to the total chlorophyll pool ranged from 5 to 99% and 1 to 95%, respectively (Fig. 4b). During bloom periods (except the 1st bloom), the contribution of microphytoplankton to the chlorophyll pool ranged from 60 to 90%.

FlowCAM data revealed that the phytoplankton densities ranged from a low of 0.0003×10^6 cells l^{-1} to a high of 1.22×10^6 cells l^{-1} (Fig. 4a). The phytoplankton abundance observed during 6 chlorophyll peaks (bloom periods) ranged from 0.004×10^6 to 1.22×10^6 cells l^{-1}. The maximum phytoplankton abundance was observed during the later stages of the monsoon period. Among the phytoplankton community, diatoms ranged up to 1.22×10^6 cells l^{-1}, dinoflagellates ranged up to 0.011×10^6 cells l^{-1}, and others (phytoflagellates) ranged up to 0.008×10^6 cells l^{-1} (Fig. 4a). In general, diatoms (82%) followed by dinoflagellates (10%) were the dominant components of the studied portion of the phytoplankton community.

The 1st bloom was observed from 31 May to 4 June. FlowCAM analysis revealed the dominance of *Navicula* and *Thalassionema* in the studied portion of the community. However, the size fractionation analysis revealed that <20 µm phytoplankton (nano- and picophytoplankton) were the most important contributors to the chlorophyll peak. The 2nd bloom was observed from 24–28 June. Microphytoplankton (*Ditylum*, *Odontella*, *Leptocylindrus* and *Thalassionema*) dominated in this bloom. The variation in the phytoplankton abundance coincided with fluctuations in salinity. The 3rd bloom was observed on 14 July and was dominated by *Skeletonema*. The 4th bloom was observed from 20–23 August. This bloom was caused by *Asterionellopsis*, *Bacteriastrum*, *Chaetoceros*, *Ditylum*, *Fragilariopsis*, *Leptocylindrus*, *Pseudo-nitzschia*, *Skeletonema*, *Thalassionema* and flagellates. The 5th and 6th blooms were observed from 1–6 and 28–30 September and were also dominated by the same species as the 4th bloom (except *Asterionellopsis*).

Relationship between environment and phytoplankton

The results of the correlation analysis and CCA are presented in Table 1 and Fig. 5, respectively. In the first CCA biplot, the 2 axes explained 98% of the

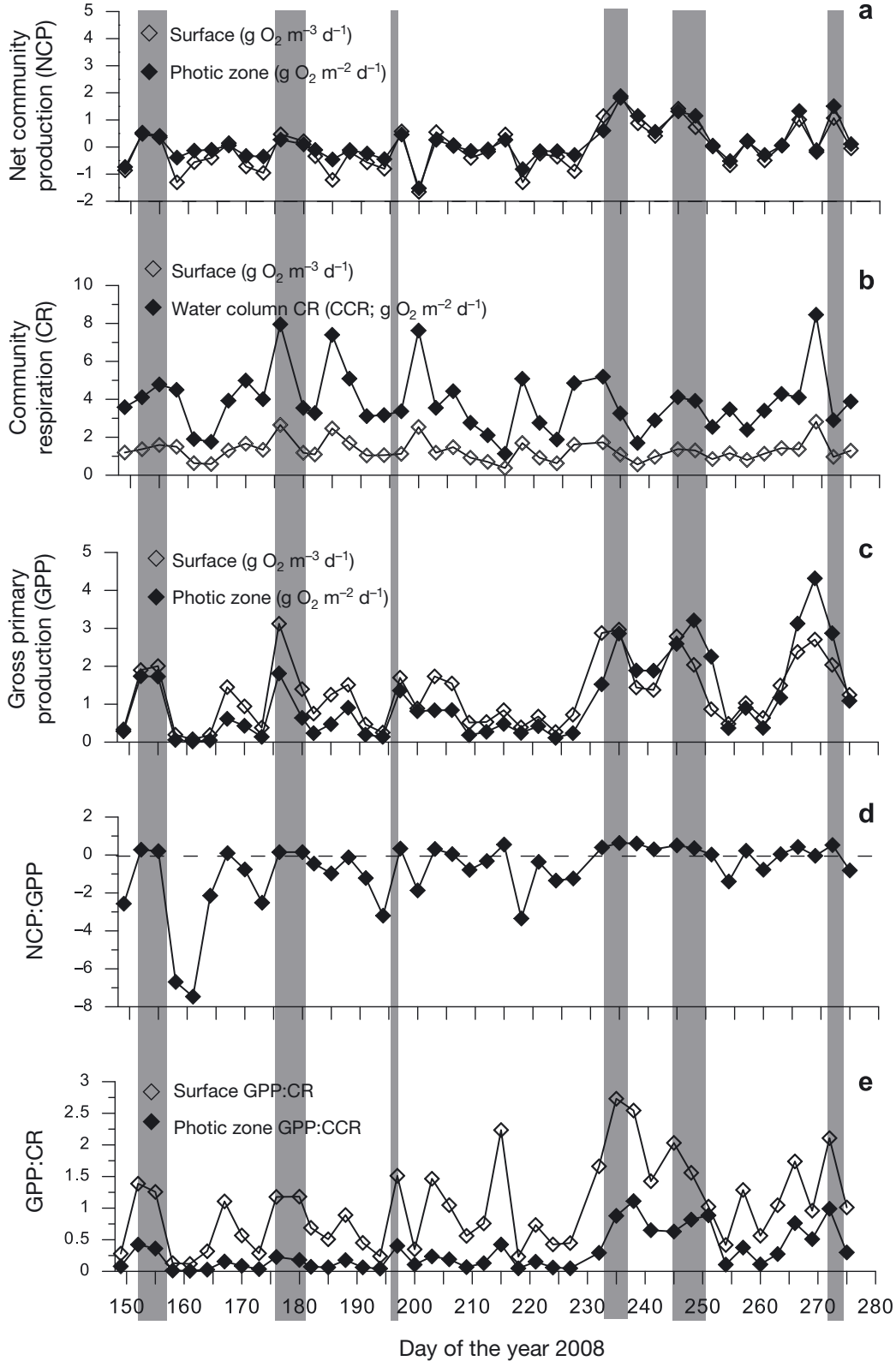

Fig. 3. Temporal variations in surface and depth-integrated metabolic rates (production and respiration rates) during the 2008 southwest monsoon: (a) surface and photic zone net community production (NCP); (b) surface (CR) and water column (CCR) community respiration; (c) surface and photic zone gross primary production (GPP); (d) surface NCP:GPP ratio; and (e) surface GPP:CR ratio and photic GPP:CCR ratio. Shaded areas in light gray represent periods of chlorophyll peaks

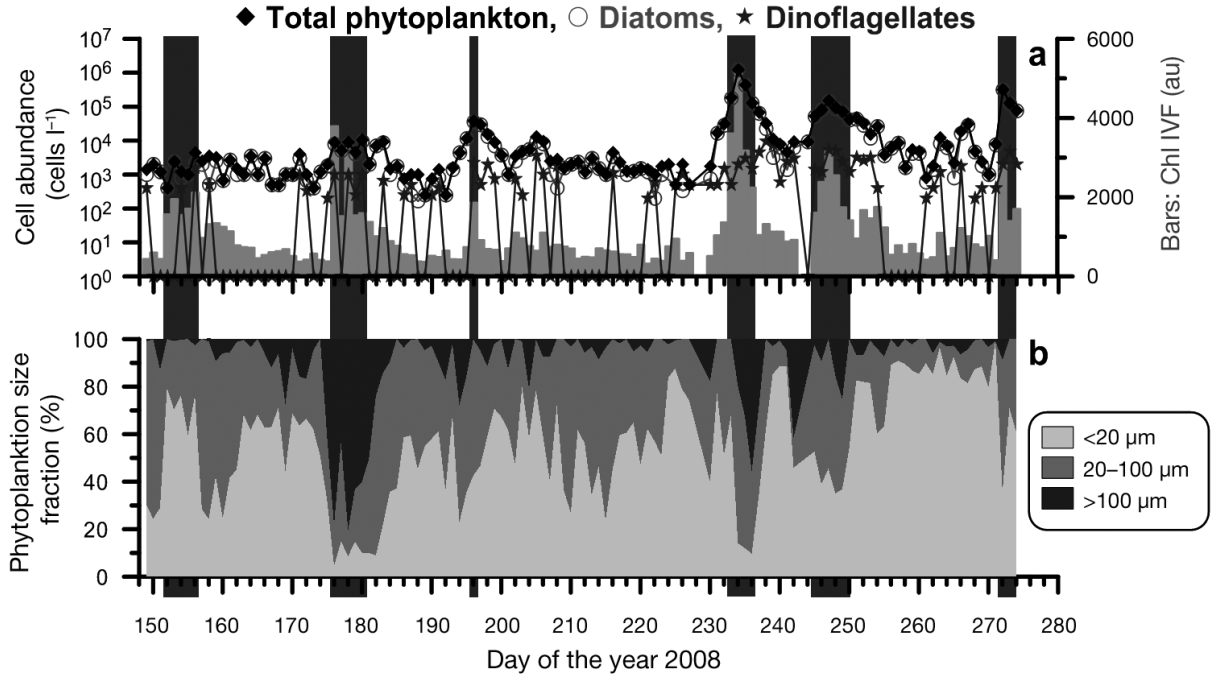

Fig. 4. Daily variations in (a) chlorophyll *in vivo* fluorescence (IVF) and abundance data of total phytoplankton, diatoms and dinoflagellates; and (b) phytoplankton size fractions (area graph), during the 2008 southwest monsoon period. Shaded areas in dark gray represent periods of chlorophyll peaks

Table 1. Spearman's rank correlation test between environmental variables and chlorophyll fluorescence, total phytoplankton and dominant phytoplankton group's abundance. Significant combinations ($p < 0.05$) are shown in **bold**

Parameter	Chlorophyll fluorescence		Diatoms		Dinoflagellates		Total phytoplankton	
	R	p	R	p	R	p	R	p
Temperature	0.13	0.141	0.12	0.202	0.05	0.581	0.05	0.555
Salinity	**0.32**	**0.001**	0.07	0.442	0.07	0.419	0.04	0.648
Secchi disc depth	**0.31**	**0.001**	**0.52**	**0.001**	**0.52**	**0.001**	**0.56**	**0.001**
Turbidity	**–0.27**	**0.003**	**–0.54**	**0.001**	**–0.56**	**0.001**	**–0.56**	**0.001**
Dissolved oxygen	0.14	0.120	0.13	0.142	0.03	0.767	0.11	0.234
Oxygen saturation	–0.04	0.635	0.02	0.833	–0.05	0.572	0.05	0.593
Rainfall	**–0.24**	**0.007**	**–0.27**	**0.003**	**–0.30**	**0.001**	**–0.23**	**0.011**
Wind speed	**–0.33**	**0.001**	**–0.41**	**0.001**	**–0.42**	**0.001**	**–0.44**	**0.001**
Solar radiation	0.14	0.116	**0.32**	**0.001**	**0.30**	**0.001**	**0.29**	**0.001**
Sunshine hours	0.14	0.127	**0.31**	**0.001**	**0.25**	**0.006**	**0.26**	**0.004**
Ammonia	–0.26	0.099	**–0.43**	**0.006**	**–0.48**	**0.002**	**–0.40**	**0.010**
Nitrate	**–0.57**	**0.001**	**–0.41**	**0.008**	**–0.55**	**0.001**	**–0.55**	**0.001**
Nitrite	–0.24	0.140	–0.25	0.116	**–0.54**	**0.001**	–0.27	0.088
Phosphate	**–0.34**	**0.032**	**–0.44**	**0.004**	**–0.69**	**0.001**	**–0.52**	**0.001**
Silicate	–0.29	0.067	–0.08	0.614	**–0.34**	**0.031**	–0.14	0.376

relationship between the phytoplankton and environmental conditions (without nutrients), whereas in the second CCA biplot, the 2 axes explained 97% of the relationship between the phytoplankton and dissolved nutrients. The results revealed that salinity, water transparency and nutrients (mainly nitrate and phosphate) are the most important environmental variables influencing the phytoplankton (chlorophyll and composition). The first CCA biplot (Fig. 5a) revealed that the water transparency (turbidity) and depth of light penetration (Secchi disc depth) are the major factors influencing the phytoplankton (chlorophyll, and abundance of total phytoplankton and dinoflagellates). Spearman's rank test revealed a significant correlation between the phytoplankton and water transparency (positive with Secchi disc depth

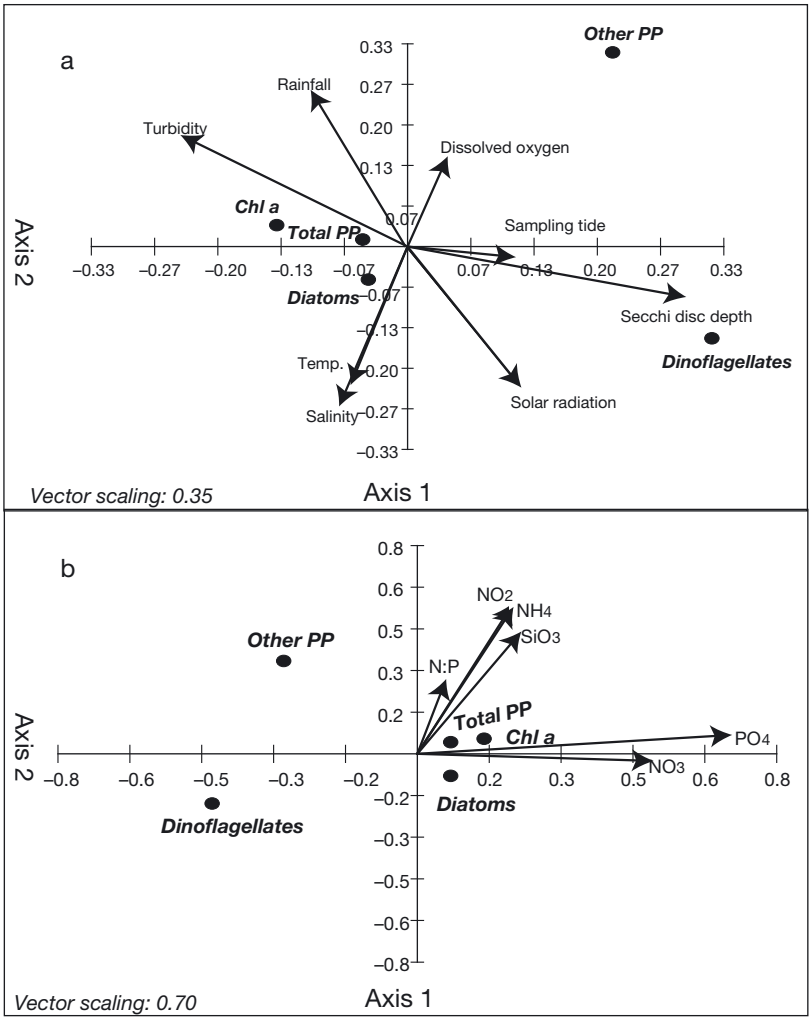

Fig. 5. Ordination diagrams for chlorophyll fluorescence and abundance (total phytoplankton, diatoms and dinoflagellates) based on canonical correspondence analysis for (a) biological and environmental data (temperature, salinity, dissolved oxygen, Secchi disc depth, turbidity, solar radiation, sampling tide and rainfall) and (b) biological and nutrients data (NH_4, NO_3, NO_2, PO_4, N:P ratio, and SiO_3). PP: phytoplankton

and negative with turbidity measurements). The CCA biplot also revealed that salinity is an important factor influencing the diatoms. However, Spearman's rank test revealed insignificant positive correlation between all the phytoplankton data and salinity (Table 1). The optimal ranges of different environmental parameters for the occurrence of high chlorophyll and abundance (total phytoplankton, diatoms and dinoflagellates) are as follows: tidal amplitude: 1.5 to 2.5 m (which corresponds to flood tide or high tide); temperature: 26 to 31°C; salinity: >15; depth of light penetration: >50 cm (for dinoflagellates: >100 cm); wind speed: <10.8 ms^{-1}; rainfall: <50 mm; and solar radiation: 30 to 70 mW cm^{-2} (Figs. 6–8). The second CCA biplot, which explains the relationship between phytoplankton and dissolved nutrients, revealed that nitrate and phosphate are the major factors influencing chlorophyll and phytoplankton abundance (both diatoms and dinoflagellates) (Fig. 5b). Spearman's test showed a significant negative correlation between phytoplankton biomass and nutrients (nitrate and phosphate), indicating the utilization of the nutrients by phytoplankton (Table 1). The ranges of nutrient concentrations, which coincided with high chlorophyll and abundance (total phytoplankton, diatoms and dinoflagellates) are as follows: nitrate < 4 µM; phosphate < 1.7 µM; and silicate < 50 µM (Figs. 6–8).

DISCUSSION

During the SWM season, the surplus freshwater discharge from the Zuari River and precipitation are added to Dona Paula Bay, resulting in marked changes in salinity field, water transparency and nutrient influx (Fig. 2a,b,d). Irrespective of the tidal conditions, the observed daily variations in salinity and rainfall indicated that the freshwater discharge and precipitation are not continuous (Fig. 2a) in the study region. The variation in salinity field is due to the episodes of high runoff followed by a lull in runoff (Vijith et al. 2009). In the present investigation, salinity of <5 was observed only during August and early September (Fig. 2a), implying high runoff at this time. During the rest of the season, the variations observed were due to the usual estuarine processes. In this study, the frequencies of changes were large and the duration for each change varied (a few to several days). Such drastic changes in hydrodynamic characteristics influence the phytoplankton biomass and community (Fig. 4). In this study, all 6 phytoplankton blooms (mainly by diatoms) reported occurred at salinity >14 (Figs. 6 & 7). A lull in river runoff as evidenced by relatively high salinity results in longer water residence time and reduced turbidity, which provides conducive environmental conditions for de-

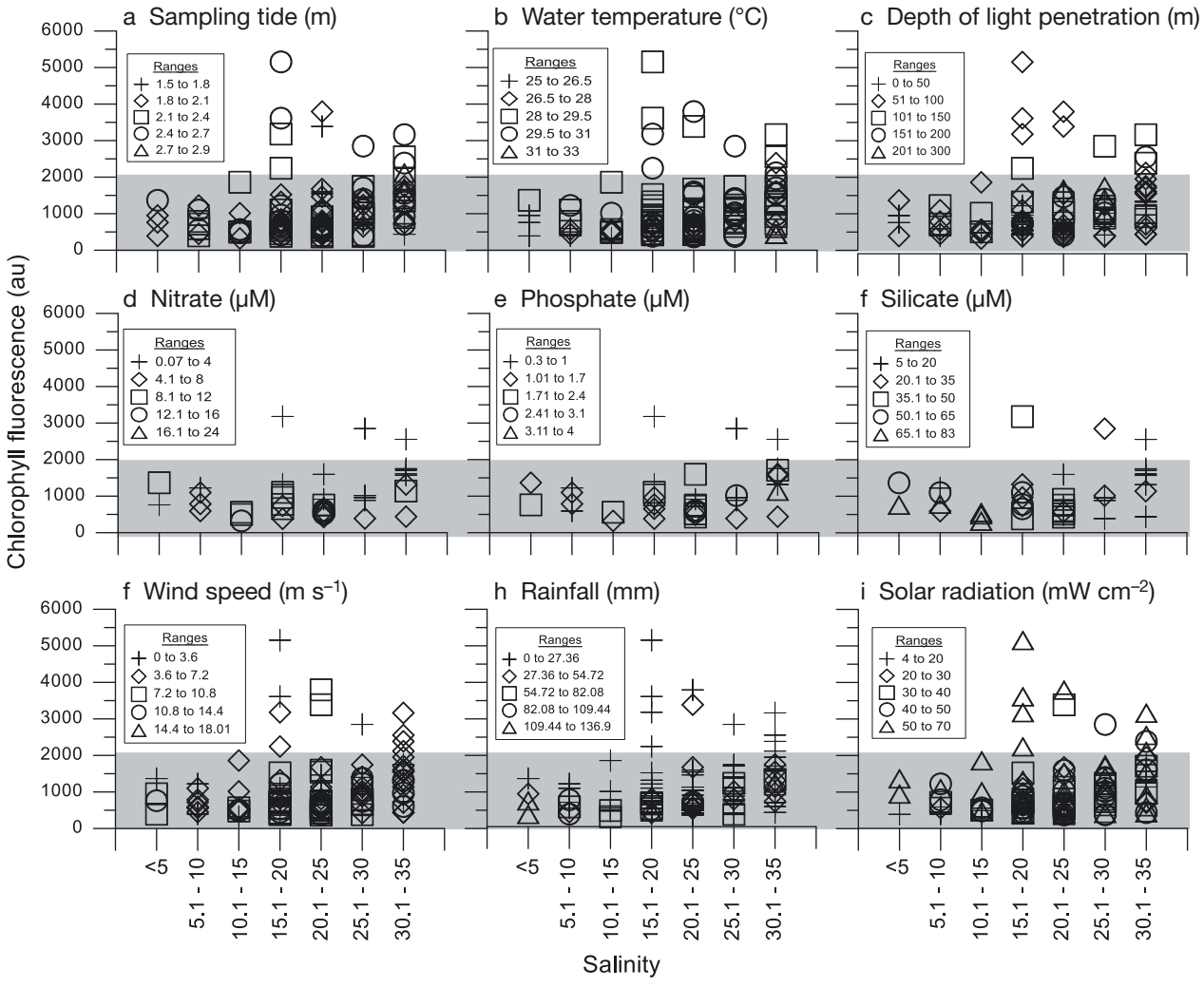

Fig. 6. Class scatter plots to derive optimal ranges of (a) sampling tide, (b) surface temperature, (c) Secchi disc depth (depth of light penetration), (d) nitrate, (e) phosphate, (f) silicate, (g) wind speed, (h) rainfall and (i) solar radiation for each salinity range (*x*-axis) and *in vivo* chlorophyll fluorescence (*y*-axis, au: arbitrary units) data points. Chlorophyll fluorescence and the corresponding environmental data were grouped based on the salinity ranges shown. Symbols above the shaded region represent chlorophyll peaks at the respective environmental range

veloping blooms of autochthonous origin (Phlips et al. 2012). Other monsoonal estuaries (Mandovi and Godavari) exhibiting varying patterns of river discharge (both natural and dam controlled) located along the Indian coast also showed similar results as observed in this study.

In the Mandovi and Zuari estuaries, the variability in salinity (due to changes in natural discharge) is large, thereby resulting in a number of peaks in phytoplankton biomass (Pednekar et al. 2011, the present study). However, in the Godavari estuary (3rd largest river in India and 60th in the world), the dam-controlled river discharge is continuous from July to December and the chlorophyll peak is associated with a decrease in discharge (Sarma et al. 2009). These observations indicate that in monsoonal estuaries, the variations in river discharge (high, moderate and low) have a bearing on the nature of phytoplankton blooms. Even in a monsoon-influenced temperate estuary (Asan Bay, Korea; Sin et al. 2012), some Australian estuaries (Eyre 2000, Ferguson et al. 2004) and the Gulf of Mexico (Murrell et al. 2007), river discharge is considered to be the main regulator of phytoplankton dynamics.

In this study, phytoplankton blooms of different duration (up to 6 d; Fig. 4a) were observed. These were caused by species belonging to different size groups. Nano- and picophytoplankton (<20 µm) dominated the first and the last (6th) blooms which occured during the beginning and the end of the monsoon (i.e.

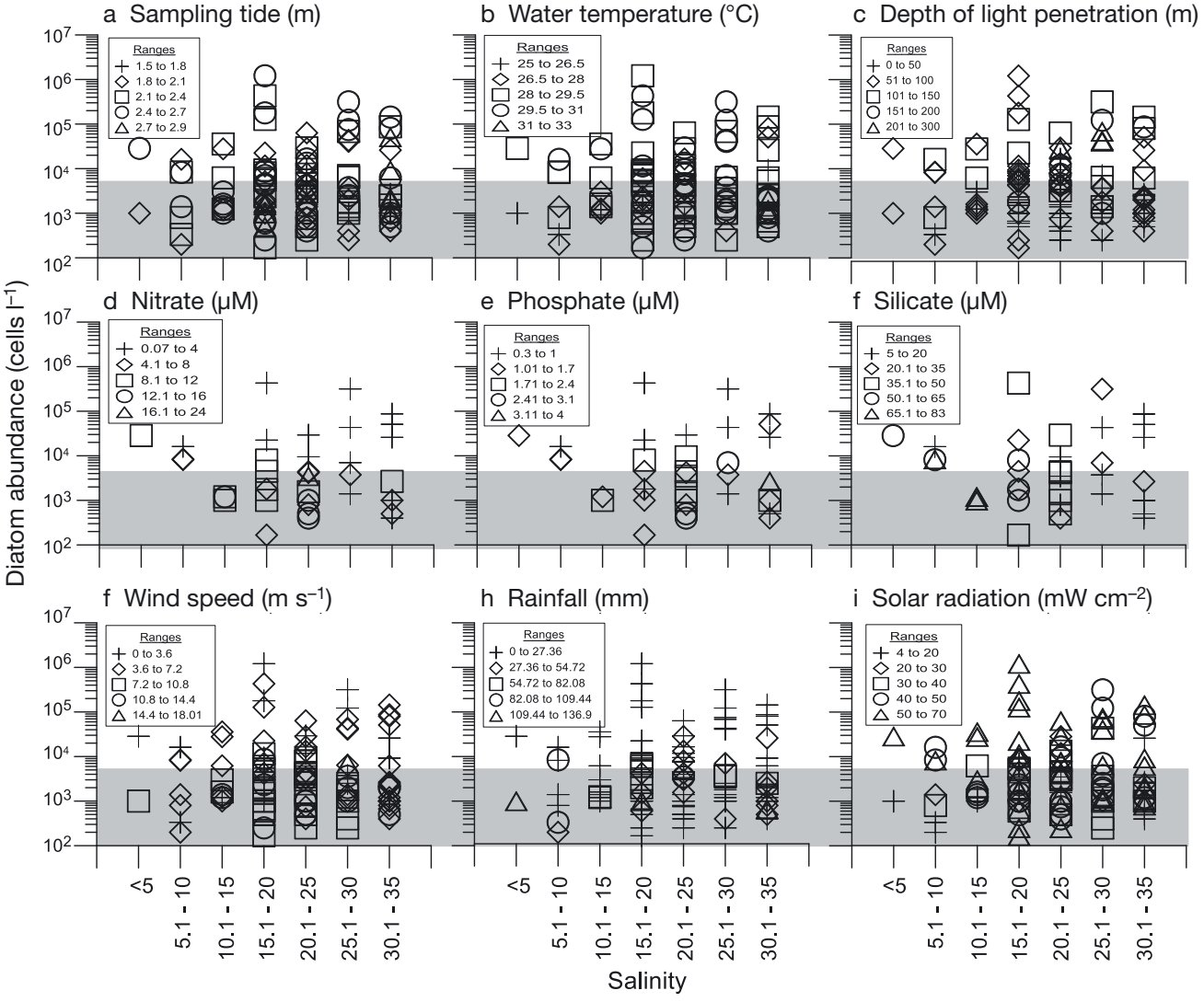

Fig. 7. As in Fig. 6, but for diatom abundance (*y*-axis)

when the salinity was >30) (Fig. 4b). In Dona Paula Bay, the picophytoplankton community is mainly represented by phycoerythrin- and phycocyanin-containing *Synechococcus* and *Prochlorococcus*-like cells and picoeukaryotes (Mitbavkar et al. 2012, 2015). The intervening blooms, which occurred in the salinity range of 14 to 30, were dominated by chain-forming and larger microphytoplankton (>20 µm). These blooms were mostly dominated by diatoms (*Asterionellopsis*, *Bacteriastrum*, *Chaetoceros*, *Ditylum*, *Fragilariopsis*, *Leptocylindrus*, *Pseudo-nitzschia*, *Skeletonema*, *Thalassionema*). The dominance of phytoplankton in each size fraction was substantiated by the FlowCAM data. Considering the tidal cycle and freshwater discharge as the major drivers for environmental perturbations in the monsoonal estuary during the monsoon, one would expect that the signals of the blooms would be short-lived. However, the fact that the blooms were observed for more than a diurnal tidal cycle indicates that they can be widespread spatially and can influence ecosystem functioning. Phytoplankton data revealed that blooms lasted for 3 to 6 d (except the 3rd bloom that was seen only for a day), indicating that blooms lasting for several days are common.

The metabolic processes such as GPP and CR are responsible for major flows of carbon in the upper waters of most aquatic systems. NCP determines whether the biological pump acts as a net source or sink of carbon (Williams 1993). An ecosystem is referred to as autotrophic if production > respiration, or heterotrophic if production < respiration. In this

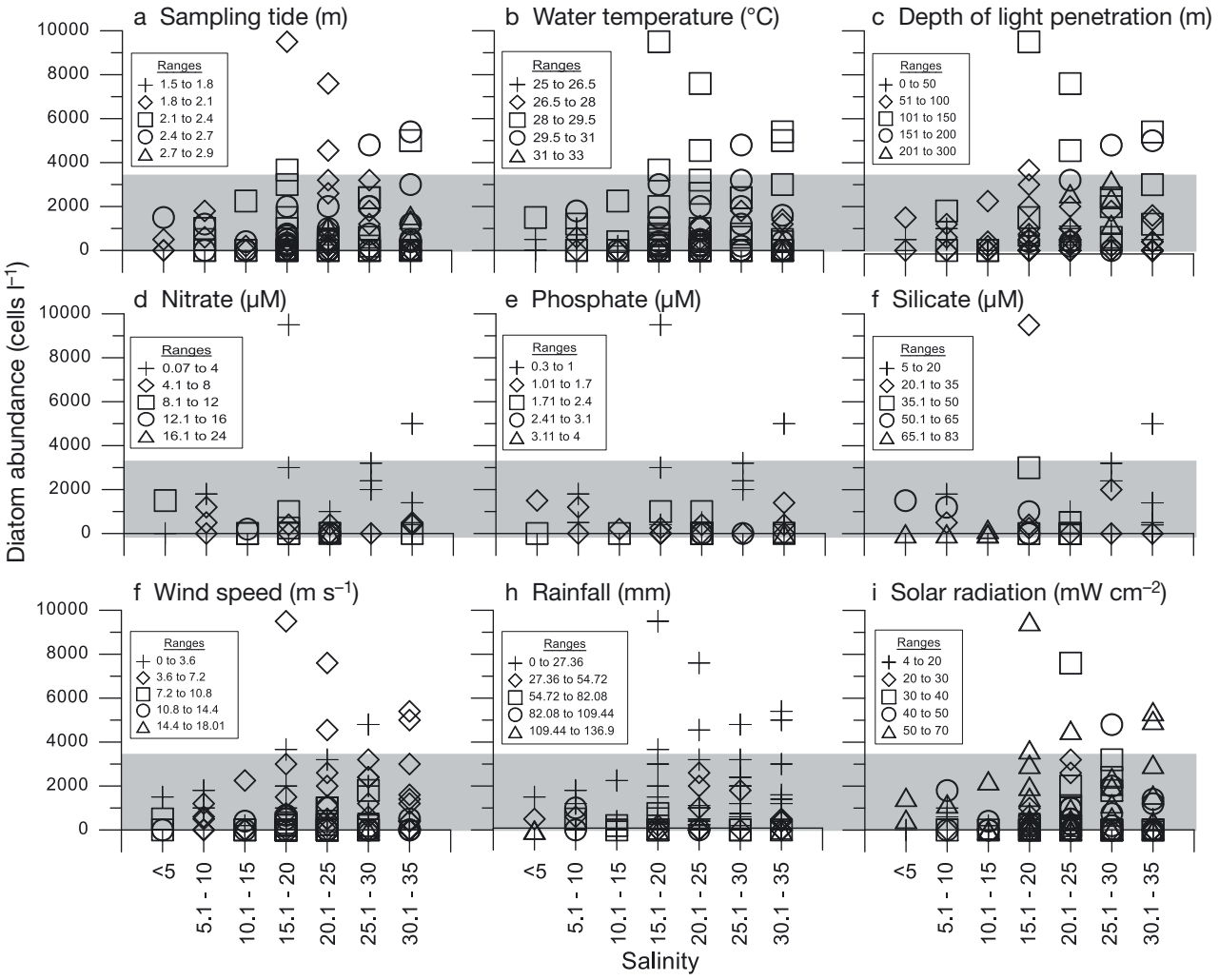

Fig. 8. As in Fig. 6, but for dinoflagellate abundance (*y*-axis)

study, the variations in NCP suggest that net autotrophic conditions prevailed during bloom events and net heterotrophic conditions during non-bloom events (except on certain occasions). This is because blooms are events of rapid production and accumulation of phytoplankton biomass (Cloern 1996). The average NCP of the photic zone is positive (0.11 ± 0.67 g O_2 m^{-2} d^{-1}), and this was due to the bloom events, further pointing out that a minimum of 25% (i.e. 30 d) of the SWM are net autotrophic. The lowest production was observed during the period of peak discharge, which is characterized by high turbidity, low water transparency and very low salinity. The reduced productivity due to high turbidity is also observed in several estuaries (Soetaert & Herman 1995, Young & Huryn 1996, Cotner et al. 2000), including monsoonal estuaries (Thottathil et al. 2008, Sarma et al. 2009), which are presently experiencing increased anthropogenic pressure. It was also observed that maximum GPP corresponded with high CR values during low phytoplankton biomass. During high biomass periods, GPP corresponded with high NCP values. The ratio of NCP:GPP was positive in the photic zone (0.02 to 0.63) during bloom events, indicating that up to 63% of the exportable production is lost in the system either by sinking, remineralization or flushing. During other (non-bloom) periods, the NCP:GPP ratio was negative (–7.47 to –0.04), indicating that *in situ* production is not sufficient to meet system requirements. During non-bloom periods, phytoplankton biomass and oxygen saturation were low, indicating low PP. The GPP:CCR ratio reveals that the *in situ* production (autochthonous supply) sustains up to 30% of the carbon requirement and the rest (up to 70%) is met by allochthonous input and benthic resuspension of the

unutilized export production. The increase in allochthonous supply results in enhanced heterotrophic respiration and reduced PP (Ram et al. 2003), whereas the benthic resuspension of the unutilized export production (mostly by phytoplankton benthic cells) characterized by low photosynthetic activity might serve as a seed source for the nature and composition of the phytoplankton bloom. In the study region, the decline in blooms, due to a decrease in nitrate concentrations and salinity change, coincided with an increase in the abundance of benthic cells (Patil & Anil 2008), which served as a seed source for subsequent blooms.

CCA revealed that the variations in salinity, rainfall, water transparency, light and nutrients play an important role in determining the nature of phytoplankton blooms and composition (Fig. 5). The variations in the environmental parameters are dependent on the magnitude of river runoff. During high runoff, the freshwater input lowers the salinity. Furthermore, freshwater brings with it nutrients and sediments to the estuary. At the same time, however, low light availability and water residence time during periods of high runoff inhibit phytoplankton growth. When runoff decreases, turbidity begins to decrease and both salinity and water residence time increase. All the blooms observed here coincided with an increase in water transparency and availability of nutrients, i.e. during the lull periods following substantial runoff events. The Secchi disc depth measurements and the phytoplankton (both chlorophyll and abundance) data revealed that a minimum of 50 cm depth of light penetration is essential for bloom formation in nutrient-rich waters (Figs. 6–8). In all 6 bloom events, the decline in the bloom coincided with low nutrient concentrations, especially nitrate, indicating the utilization of nutrients by the bloom (Fig. 2d). Recruitment of cells from the bottom sediments can also be an important factor in bloom formation (Underwood & Kromkamp 1999). Some studies have also reported that exchange of algal cells between the benthos and water column can be significant in estuaries like the Ems (de Jonge & van Beusekom 1995) and the Gironde (Irigoien & Castel 1997). Benthic propagules repopulate waters if resuspended and exposed to suitable light, temperature and nutrients (McQuoid et al. 2002). Since the study site is shallow, freshwater discharge can cause resuspension of diatom benthic propagules. The resuspended benthic propagules might then seed the subsequent blooms under suitable environmental conditions. Probably this process could be the reason for the occurrence of a multi-species (*Bacteriastrum*, *Chaetoceros*, *Ditylum*, *Fragilariopsis*, *Leptocylindrus*, *Pseudo-nitzschia*, *Skeletonema*, *Thalassionema*) bloom thrice on different occasions (20–23 August, 1–6 and 28–30 September).

The second most abundant group, the dinoflagellates, was also influenced by variations in salinity, rainfall, wind speed, water transparency, light and nutrients (Fig. 5). In one of our earlier studies, during the bloom period, cell abundance ranged to up to 9×10^4 cells l^{-1} (Patil & Anil 2011); however, in the present study, the maximum cell abundance recorded was 9.5×10^3 cells l^{-1}. In view of this, it is presumed that the dinoflagellate blooms were not observed in the present study, even though they contributed more than diatoms on certain occasions. A noteworthy observation was that the increase in dinoflagellate abundance was associated with an increase in water transparency (>100 cm), solar radiation (30–70 mW cm^{-1}) and low nutrient concentrations (Fig. 8). This is the first such observation for this region. The increase in dinoflagellate population during the end of the monsoon and the beginning of post-monsoon (periods characterized by increased water transparency and salinity) was also reported in the Mandovi estuary, which, with the Zuari River and Cumbarjua canal, forms the major estuarine system of the region (Pednekar et al. 2011). Although HAB dinoflagellates such as *Gymnodinium* (up to 800 cells l^{-1}, occurred on 6 occasions) and *Cochlodinium* (200 to 500 cells l^{-1}, occurred on 2 occasions) were encountered, they did not cause blooms as reported during the 2000 monsoon (Patil & Anil 2011). The break in rainfall during the 2000 monsoon (July) coincided with a bloom of these organisms under high-saline, nutrient-poor and transparent water-column (Secchi disc depth: 245 cm) conditions (Patil & Anil 2011). However, such conditions did not occur during the present study, indicating that interannual variations and monsoon-influenced perturbations play an important role in the occurrences of blooms.

In summary, this study provides insights into phytoplankton bloom formation during the SWM based on high-resolution observations of live phytoplankton cells and environmental parameters from a tropical estuary. Environmental data revealed that during SWM, the study region experiences significant variations in wind speed, turbidity and light conditions, water residence time and freshwater inputs (river and precipitation) with associated salinity and nutrient dynamics at time scales of days to weeks. Under such conditions, several phytoplankton blooms lasting for >1 d occurred, indicating that such events are widespread and can influence the

metabolic balance of the ecosystem. These blooms occurred when there was a lull in runoff under favorable conditions. All of the blooms coincided with flood tide or high tide under salinity conditions of >15 and specific light (depth of light penetration: >50 cm; solar radiation: 30–70 mW cm^{-2}) conditions following heavy rainfall and nutrient flux. In addition, dinoflagellate abundance was noted to increase with an increase in the depth of light penetration (>100 cm) and at low nutrient concentrations. We conclude that the cyclicity and the characteristics of the intraseasonal phytoplankton blooms in monsoonal estuaries are governed by the intensity and length of the perturbations.

Acknowledgements. We thank the Director of CSIR-NIO for support and encouragement. We thank Mr. D. Sundar for providing tidal amplitude data using the tidal analysis software kit (TASK-2000) during the sampling time. We thank the Water Resource Department, Government of Goa, Goa, India, and Dr. Prakash Mehra of Marine Instrumentation Department, CSIR-NIO, Goa, India, for providing the river discharge and AWS data. We are also thankful to the 3 anonymous reviewers for their suggestions in improving the manuscript. J.S.P. acknowledges the Department of Science and Technology, Government of India for the award of the SERC young scientist project. This paper is NIO contribution no. 5734.

LITERATURE CITED

Acharyya T, Sarma VVSS, Sridevi B, Venkataramana V and others (2012) Reduced river discharge intensifies phytoplankton bloom in Godavari estuary, India. Mar Chem 132–133:15–22

Álvarez E, López-Urrutia A, Nogueira E, Fraga S (2011) How to effectively sample the plankton size spectrum? A case study using FlowCAM. J Plankton Res 33:1119–1133

Benson BB, Krause D Jr (1984) The concentration and isotopic fractionation of oxygen dissolved in freshwater and seawater in equilibrium with the atmosphere. Limnol Oceanogr 29:620–632

Bhattathiri PMA, Devassy VP, Bhargava RMS (1976) Production at different trophic levels in the estuarine system of Goa. Indian J Mar Sci 5:83–86

Cloern EJ (1979) Phytoplankton ecology of the San Francisco Bay system: the status of our current understanding. In: San Francisco Bay: the urbanized estuary. Pacific Division of American Association for the Advancement of Science, California Academy of Sciences, San Francisco, CA, p 247–264

Cloern EJ (1996) Phytoplankton bloom dynamics in coastal ecosystems: a review with some general lessons from sustained investigation of San Francisco Bay, California. Rev Geophys 34:127–168

Cloern EJ, Jassby AD (2010) Patterns and scales of phytoplankton variability in estuarine–coastal ecosystems. Estuar Coast 33:230–241

Cloern EJ, Jassby AD (2012) Drivers of change in estuarine-coastal ecosystems: discoveries from four decades of study in San Francisco Bay. Rev Geophys 50:RG4001, doi:10.1029/2012RG000397

Cole JJ, Caraco NF, Peierls BL (1992) Can phytoplankton maintain a positive carbon balance in a turbid, freshwater, tidal estuary? Limnol Oceanogr 37:1608–1617

Conley D (2000) Biogeochemical nutrient cycles and nutrient management strategies. Hydrobiologia 410:87–96

Cotner JB, Johengen TJ, Biddanda BA (2000) Intense winter heterotrophic production stimulated by benthic resuspension. Limnol Oceanogr 45:1672–1676

de Jonge V, van Beusekom J (1995) Wind- and tide-induces resuspension of sediment and microphytobenthos from tidal flats in the Ems estuary. Limnol Oceanogr 40: 766–778

Desikachary TV (1987) Diatom flora of some sediments from the Indian Ocean Region. In: Atlas of diatoms, Fascicle II. T T Maps and Publications Private Limited, Chrompet, Madras, p 1–10

Devassy VP, Goes JI (1988) Phytoplankton community structure and succession in a tropical estuarine complex (central west coast of India). Estuar Coast Shelf Sci 27: 671–685

Eyre BD (2000) Regional evaluation of the nutrient transformation and phytoplankton growth in nine river-dominated sub-tropical east Australian estuaries. Mar Ecol Prog Ser 205:61–83

Eyre BD, Ferguson AJP (2006) Impact of a flood event on benthic and pelagic coupling in a sub-tropical east Australian estuary (Brunswick). Estuar Coast Shelf Sci 66: 111–122

Ferguson AJP, Eyre BD, Gay J (2004) Nutrient cycling in the sub-tropical Brunswick estuary, Australia. Estuaries 27: 1–17

Irigoien X, Castel J (1997) Light limitation and distribution of chlorophyll pigments in a highly turbid estuary: the Gironde (SW France). Estuar Coast Shelf Sci 44:507–517

Krishna Kumari L, Bhattathiri PMA, Matondkar SGP, John J (2002) Primary productivity in Mandovi-Zuari estuaries in Goa. J Mar Biol Assoc India 44:1–13

Lawrenz E, Smith EM, Richardson TL (2013) Spectral irradiance, phytoplankton community composition and primary productivity in a salt marsh estuary, North Inlet, South Carolina, USA. Estuar Coast 36:347–364

Lehman PW (1992) Environmental factors associated with long-term changes in chlorophyll concentration in the Sacramento-San Joaquin Delta and Suisun Bay, California. Estuaries 15:335–348

Malone TC, Crocker LH, Pike SE, Wendler BW (1988) Influences of river flow on the dynamics of phytoplankton production in a partially stratified estuary. Mar Ecol Prog Ser 48:235–249

McQuoid MR, Godhe A, Nordberg K (2002) Viability of phytoplankton resting stages in the sediments of a coastal Swedish fjord. Eur J Phycol 37:191–201

Mitbavkar S, Anil AC (2002) Diatoms of the microphytobenthic community: population structure in a tropical intertidal sand flat. Mar Biol 140:41–57

Mitbavkar S, Rajaneesh KM, Anil AC, Sundar D (2012) Picophytoplankton community in a tropical estuary: detection of *Prochlorococcus*-like populations. Estuar Coast Shelf Sci 107:159–164

Mitbavkar S, Patil JS, Rajaneesh KM (2015) Picophytoplankton as tracers of environmental forcing in a tropical monsoonal bay. Microb Ecol, doi:10.1007/s00248-015-0599-2

Murrell MC, Hagy JD III, Lores EM, Greene RM (2007)

Phytoplankton production and nutrient distributions in a subtropical estuary: importance of freshwater flow. Estuar Coast 30:390–402

Naqvi SWA, Jayakumar DA, Narvekar PV, Naik H and others (2000) Increased marine production of N_2O due to intensifying anoxia on the Indian continental shelf. Nature 408:346–349

Nowicki BL, Nixon SW (1985) Benthic nutrient remineralization in a coastal lagoon ecosystem. Estuaries 8:182–190

Paerl HW (1997) Coastal eutrophication and harmful algal blooms: importance of atmospheric deposition and groundwater as 'new' nitrogen and other nutrient sources. Limnol Oceanogr 42:1154–1165

Parsons TR, Maita Y, Lalli CM (1984) A manual of chemical and biological methods for seawater analysis. Pergamon Press, Oxford

Patil JS, Anil AC (2008) Temporal variation of diatom benthic propagules in a monsoon-influenced tropical estuary. Cont Shelf Res 28:2404–2416

Patil JS, Anil AC (2011) Variations in phytoplankton community in a monsoon influenced tropical estuary. Environ Monit Assess 182:291–300

Pednekar SM, Matondkar SGP, Gomes HDR, Goes JI, Parab S, Kerkar V (2011) Fine-scale responses of phytoplankton to freshwater influx in a tropical monsoonal estuary following the onset of southwest monsoon. J Earth Syst Sci 120:545–556

Pennock JR (1985) Chlorophyll distribution in the Delaware estuary: regulation by light limitation. Estuar Coast Shelf Sci 21:711–725

Phlips EJ, Badylak S, Hart J, Haunert D and others (2012) Climatic influences on autochthonous and allochthonous phytoplankton blooms in a subtropical estuary, St. Lucie estuary, Florida, USA. Estuar Coast 35:335–352

Qasim SZ, SenGupta R (1981) Environmental characteristics of the Mandovi-Zuari estuarine system in Goa. Estuar Coast Shelf Sci 13:557–578

Ram ASP, Nair S, Chandramohan D (2003) Seasonal shift in net ecosystem production in a tropical estuary. Limnol Oceanogr 48:1601–1607

Rao VP, Shynu R, Kessarkar PM, Sundar D and others (2011) Suspended sediment dynamics on a seasonal scale in the Mandovi and Zuari estuaries, central west coast of India. Estuar Coast Shelf Sci 91:78–86

Round FE, Crawford RM, Mann DG (1990) The diatoms: biology and morphology of the genera. Cambridge University Press, New York, NY

Sarma VVSS, Gupta SNM, Babu PVR, Acharya T and others (2009) Influence of river discharge on planktonic metabolic rates in the tropical monsoon driven Godavari estuary, India. Estuar Coast Shelf Sci 85:515–524

Sarma VVSS, Prasad VR, Kumar BSK, Rajeev K and others (2010) Intra-annual variability in nutrients in the Godavari estuary, India. Cont Shelf Res 30:2005–2014

Sin Y, Wetzel RL, Anderson IC (1999) Spatial and temporal characteristics of nutrient and phytoplankton dynamics in the York River Estuary, Virginia: analyses of long-term data. Estuaries 22:260–275

Sin Y, Hyun B, Bach QD, Yang S, Park C (2012) Phytoplankton size and taxonomic composition in a temperate estuary influenced by monsoon. Estuar Coast 35:839–852

Soetaert K, Herman PMJ (1995) Nitrogen dynamics in the Westershelde estuary (SW Netherlands) estimated by means of the ecosystem model MOSES. Hydrobiologia 311:225–246

Subrahmanyan R (1959) Studies on the phytoplankton of the west coast of India, Parts I and II. Proc Ind Acad Sci 50B: 113–187

Thottathil SD, Balachandran KK, Gupta GVM, Madhu NV, Nair S (2008) Influence of allochthonous input of autotrophic-heterotrophic switch-over in shallow waters of a tropical estuary (Cochin Estuary), India. Estuar Coast Shelf Sci 78:551–562

Tomas CR (1997) Identifying marine phytoplankton. Academic Press, New York, NY

Underwood GJC, Kromkamp J (1999) Primary production by phytoplankton and microphytobenthos in estuaries. Adv Ecol Res 29:94–153

Vijith V, Sundar D, Shetye SR (2009) Time-dependence of salinity in monsoonal estuaries. Estuar Coast Shelf Sci 85:601–608

Vinagre C, Salgado J, Cabral HN, Costa MJ (2011) Food web structure and habitat connectivity in fish estuarine nurseries — impact of river flow. Estuar Coasts 34:663–674

Williams PJleB (1993) On the definition of plankton terms. ICES Mar Sci Symp 197:9–19

Young RG, Huryn AD (1996) Inter-annual variation in discharge controls ecosystem metabolism along a grassland river continuum. Can J Fish Aquat Sci 53:2199–2211

Zarauz L, Irigoien X (2008) Effects of Lugol's fixation on the size structure of natural nano–microplankton samples, analyzed by means of an automatic counting method. J Plankton Res 30:1297–1303

Zingone A, Phlips EJ, Harrison PJ (2010) Multiscale variability of twenty-two coastal phytoplankton time series: a global comparison. Estuar Coast 33:224–229

Editorial responsibility: Katherine Richardson, Copenhagen, Denmark

Submitted: December 3, 2013; Accepted: March 18, 2015
Proofs received from author(s): June 10, 2015